Investigation on critical equilibrium of trapped air pocket in water supply pipeline system[*]

Wu-yi WAN[†1,2], Chen-yu LI[1], Yun-qi YU[1]

(*[1]Department of Hydraulic Engineering, College of Civil Engineering and Architecture, Zhejiang University, Hangzhou 310058, China*)
(*[2]State Key Laboratory of Hydraulic Engineering Simulation and Safety, Tianjin University, Tianjin 310072, China*)
[†]E-mail: wanwuyi@zju.edu.cn

Abstract: A trapped air pocket can cause a partial air lock in the top of a hump pipe zone. It increases the resistance and decreases the hydraulic cross section, as well as the capacity of the water supply pipeline. A hydraulic model experiment is conducted to observe the deflection and movement of the trapped air pocket in the hump pipe zone. For various pipe flow velocities and air volumes, the head losses and the equilibrium slope angles are measured. The extra head losses are also obtained by reference to the original flow without the trapped air pocket. Accordingly, the equivalent sphere model is proposed to simplify the drag coefficients and estimate the critical slope angles. To predict the possibility and reduce the risk of a hump air lock, an empirical criterion is established using dimensional analysis and experimental fitting. Results show that the extra head losses increase with the increase of the flow velocity and air volume. Meanwhile, the central angle changes significantly with the flow velocity but only slightly with the air volume. An air lock in a hump zone can be prevented and removed by increasing the pipe flow velocity or decreasing the maximum slope of the pipe.

1 Introduction

In an irregular submarine water supply pipeline system, air can remain and accumulate at the top of a hump zone when the pipe flow velocity is not large enough to remove it. The trapped air pocket in the hump can obstruct flow and reduce the conveying capacity of the pipe (Pozos *et al.*, 2010). Consequently, this kind of local hydraulic phenomenon is also called an air lock (Greenshields and Leevers, 1995; Reynolds and Yitayew, 1995; Brown, 2006). It is a problem in irrigation and drainage systems (Zhou *et al.*, 2004; Burch and Locke, 2012; Pozos-Estrada *et al.*, 2015), hydraulic spillway conduits (Liu and Yang, 2013), and water pipeline systems (Burrows and Qiu, 1995; Carlos *et al.*, 2011; Pozos-Estrada *et al.*, 2012), since it increases the head losses, decreases the cross section, and causes pipe burst failures. According to the scale of the air lock, it can be classified as an entire air lock or a partial air lock (Brown, 2006). Generally, an entire air lock occurs in small-scale pipes. It increases significantly the head losses in the pipe flow, and even partially or entirely blocks the pipe flow in low-pressure gravity flow pipe systems (Reynolds and Yitayew, 1995). For storm sewer and water supply pipe systems, the trapped air usually forms a partial air lock even if it does not entirely block the hydraulic cross section of the closed pipe (Yu, 2015). However, the trapped air mass can cause pressure oscillations (Vasconcelos and Leite, 2012), increase the transient pressure peak (Burrows and

Qiu, 1995; Chaiko and Brinckman, 2002), and cause burst failures (Zhou *et al.*, 2004; Pozos-Estrada *et al.*, 2015) in some closed pipeline systems.

To avoid the hazard of air locks, various air lock categories and their hydraulic properties have been investigated in the last few years (Pothof and Clemens, 2011; Pozos-Estrada *et al.*, 2012). Reynolds and Yitayew (1995) studied the air lock phenomenon of a low head irrigation pipeline, with small internal diameters of 6, 8, 10, and 13 mm, and the results show that an entire air lock can form a partial or full blockage in a small-scale pipe. Pozos *et al.* (2010) studied the equilibrium and movement of air pockets in gravity and pumping pipeline systems by hydraulic experiments. A useful evaluation criterion was established to predict the motion direction of an air pocket in a straight downward sloping pipe. In the meantime, Pothof and Clemens (2010) provided two important clearing velocity criteria according to energy considerations and momentum balance for elongated air pockets in straight downward sloping pipes. Izquierdo *et al.* (1999) studied the influence of an air pocket in a pipe start-up. Escarameia (2007) and Lin *et al.* (2015) measured air pocket movement in a pressurized conduit pipe system. In addition, the influence of air pockets on water hammer has been widely considered by experiments and numerical simulations (Epstein, 2008; Zhou *et al.*, 2013; Ferreri *et al.*, 2014).

Previous research shows that air locks can cause undesired obstructions and pressure fluctuations in closed irrigation and pipe systems. These are significant for pipe design and water hammer protection by avoiding air pocket hazards in straight sloping pipes. However, the air lock is more complicated in the hump pipe zone than in a straight downward sloping pipe, considering that the pipe fluctuates with the irregular submarine profile. Moreover, air valves cannot be used in submarine conditions to eliminate air pockets. To prevent partial air locks in an undulating submarine water supply pipeline system, in this study the physical equilibrium and extra losses are investigated with a uniform annular circular pipe. The partial air locks have been observed by experiments and the equilibrium equations are established by dimensional analysis and force equilibrium. Considering the complexity of the trapped air pocket shape, the equivalent sphere model (ESM) is proposed to

simplify and establish a critical equilibrium relationship. Finally, an empirical criterion coefficient is proposed to evaluate the possibility of an air lock and to prevent the air lock. It provides guidance for the design of pipe slope and flow velocity to prevent and remove partial air locks in irregular submarine pipelines.

2 Basic profiles and force equilibrium of an air lock in a hump pipe zone

In closed pipe flow, bubbles always move to the top of a pipe because air is far less dense than liquid. If the drag force of a flow is not large enough to remove these bubbles, they will accumulate gradually and cause an air lock in the top of the hump pipe zone. Unfortunately, an air lock can increase the resistance and reduce the flow capacity of a closed pipe system. Sometimes, in some low-pressure pipe systems, it can even entirely block the water supply. Fig. 1 shows an entire air lock, where the air occupies the complete flow cross section. An entire air lock can greatly affect the flow capacity of a pipe. If the flow velocity and pressure difference are large enough, the air pocket will move in the same direction as the pipe flow. Conversely, it can partially or entirely block the pipe flow. Usually, this kind of phenomenon occurs only in small-scale low-pressure pipe systems as in the examples in Reynolds and Yitayew (1995) and Brown (2006). Our experiment also shows that it is difficult to observe an entire air lock in a large-scale water supply pipe with a 90-mm internal diameter.
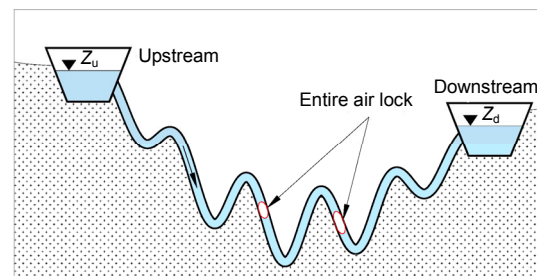

Fig. 1 Schematic of an entire air lock in a small-diameter pipe system (Z_u: upstream water level; Z_d: downstream water level)

Unlike the entire air lock, a partial air lock often occurs in large-diameter pipe systems. As shown in

Fig. 2, a partial air lock usually partially fills the pipe cross section near the top of the hump zone in a submarine water supply pipeline. The deflection and dissipation of the partial air lock are more complicated in a hump pipe than in a straight slope pipe. Therefore, we focus on a partial air lock in the hump zone, and conduct an experiment to observe and measure that partial air lock. Moreover, the critical equilibrium conditions are established by force analysis and dimensional analysis, as well as empirical fitting according to the experimental results.
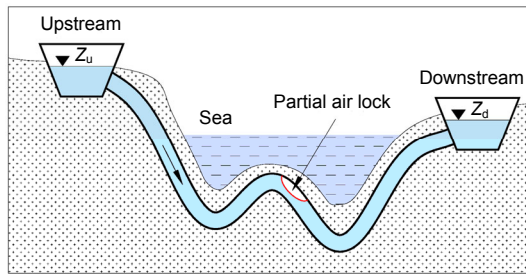

Fig. 2 Schematic of a partial air lock in a submarine water supply system (Z_u: upstream water level; Z_d: downstream water level)

In general, the shape of an air lock varies with the pipe diameter and flow velocity, as well as the hydraulic pressure (Liu and Yang, 2013; Lin *et al.*, 2015). As a typical air lock, Fig. 3 shows the basic profile observed in our experiment. The upper shape is profiled by the internal surface of the pipe wall, and the lower shape is approximately a bent flow interface. The profile of the air pocket changes with the flow velocity and pressure; therefore, it is difficult to describe accurately the shape by a regular model. To simplify the air lock, ESM is proposed in the next section to describe the trapped air pocket.
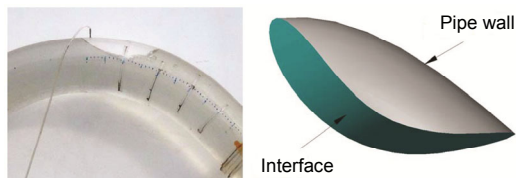

Fig. 3 Typical profile of a partial air lock in a hump

Considering the air lock as the control volume for a critical equilibrium condition, there are primarily four kinds of forces acting on the trapped air pocket, i.e., gravity, its buoyancy, the drag force of the flow, and the normal force of the pipe wall (Fig. 4). In this figure, the effect of the friction between air and pipe wall is neglected, since the viscosity of air is negligible at ordinary temperatures and pressures. For an air mass at rest, the sum of the force vectors equals zero. It can be written as follows:

$$\boldsymbol{F}+\boldsymbol{G}+\boldsymbol{D}+\boldsymbol{N}=\boldsymbol{0}, \tag{1}$$

where $\boldsymbol{D}$ is the drag force vector, $\boldsymbol{F}$ the buoyancy vector, $\boldsymbol{G}$ the gravity vector, and $\boldsymbol{N}$ the normal force of the pipe wall. In vector analysis, through vector decomposition along the radial and tangential directions in the 2D plane, the equilibrium of the tangential component can be expressed as follows:

$$\left[\begin{array}{cc}|\boldsymbol{D}| & |\boldsymbol{N}|\end{array}\right]^{\mathrm{T}} = \left[\begin{array}{cc}|\boldsymbol{F}+\boldsymbol{G}|\sin\theta & |\boldsymbol{F}+\boldsymbol{G}|\cos\theta\end{array}\right]^{\mathrm{T}}, \tag{2}$$

where θ is the central depression angle of the pocket. Therefore, the location depression angle of the air lock is

$$\theta = \arcsin\left(\frac{|\boldsymbol{D}|}{|\boldsymbol{F}+\boldsymbol{G}|}\right). \tag{3}$$

Referring to the air lock at rest, the buoyancy force can be calculated simply by Archimedes' principle:

$$F=\rho_{\mathrm{w}}gV, \tag{4}$$
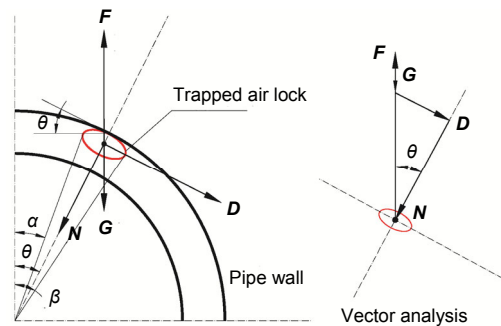

Fig. 4 Force analysis of a partial air lock in a hump
F: buoyancy vector; G: gravity vector; D: drag force vector; N: normal force; α: left depression angle; β: right depression angle; θ: central depression angle

where F is the gravity, ρ_w the water density, g the acceleration of gravity, and V the volume of the trapped air pocket. In fact, buoyancy is also the only original force driving the air lock to the top. It always provides a component force opposite to the directional flow.

The typical drag equation, originally established by Lord Rayleigh, can be expressed as

$$D = \frac{1}{2}\rho_w v^2 C_D A, \qquad (5)$$

where D is the drag force, v the mean flow velocity in the pipe, C_D the drag coefficient, and A the flow direction-projected area. Thus, combining Eqs. (4) and (5) with Eq. (3), the depression angle of the air pocket can be expressed as

$$\theta = \arcsin\left(\frac{C_D A}{V} \cdot \frac{\rho_w}{\rho_w - \rho_a} \cdot \frac{v^2}{2g}\right), \qquad (6)$$

where ρ_a is the air density. Practically, it is very difficult to determine the drag force of the flow acting on the air lock if the original shape of the trapped air pocket is considered as shown in Fig. 3. Here, an ESM is proposed to simplify the model of the trapped air pocket. In the model, the suppositional ESM is defined as: (1) a sphere equals the air pocket in volume; (2) the sphere is subjected to the same forces as the original air pocket. Then the relevant equivalent radius is

$$r^* = \sqrt[3]{0.75V/\pi}, \qquad (7)$$

where r^* is the equivalent radius of the air pocket. The projected area of the equivalent sphere in the flow section is

$$A^* = \pi\left(r^*\right)^2, \qquad (8)$$

where A^* is the equivalent section area. Based on the ESM, Eq. (6) is converted to

$$\theta = \arcsin\left(\frac{3}{4} \cdot \frac{C_D^*}{r^*} \cdot \frac{\rho_w}{\rho_w - \rho_a} \cdot \frac{v^2}{2g}\right), \qquad (9)$$

where C_D^* is the equivalent drag coefficient in the ESM. Moreover, to describe the relative scale of the air pocket to the pipe section, the dimensionless radius is defined as

$$\tilde{r} = r^* / r_0, \qquad (10)$$

where $\tilde{r}$ is the dimensionless radius of the air pocket and r_0 is the internal radius of the pipe. Then Eq. (9) is written as

$$\theta = \arcsin\left(\frac{3}{4} \cdot \frac{C_D^*}{\tilde{r}r_0} \cdot \frac{\rho_w}{\rho_w - \rho_a} \cdot \frac{v^2}{2g}\right). \qquad (11)$$

Eqs. (9) and (11) are not subject to the effects of the air pocket shape and they give an approach for establishing the drag coefficient of the equivalent sphere in the following experimental research and data analysis.

3 Experimental layout and measure principle

Generally, the critical equilibrium of the air lock in the hump is complicated, because of deformation and separation. To study the critical state of the air lock and its influence on the pipe flow, an experiment was conducted. Fig. 5 shows the schematic of the experimental principle and Fig. 6 shows the experimental facilities in the field. The experiment consists mainly of a hump pipe, with upstream and downstream pools, a slope differential manometer, an air supply measuring cylinder, and a flow control valve. The hump pipe is 0.090 m in internal diameter. The hump is 0.450 m in external radius and the angle of the hump is $\pi/2$.

In the experiment, the measurements include the volumes and the location depression angle of the air lock, the pressure, the flow velocity, and the hydraulic head losses, under various flow and air lock conditions. The volumes of the air lock are 40, 80, and 160 cm^3, and the pipe flow velocity varies from 0 to 0.7 m/s.

The head losses are very small and difficult to measure. To improve the measurement precision of the pressure difference between station 1 and station 2, a differential manometer was fixed aslant with a

specific slope. The gradient is 1:4.899; in other words, the angle is $\alpha_g=\arcsin(1/5)$. The minimum interval of the ruler is 1 mm and the corresponding measuring precision is 0.2 mm in head losses. As shown in Fig. 5, the head losses are determined as follows:

$$h_{12} = (h_{s1} - h_{s2})\sin\alpha_g - (h_{s1} - h_{s2})\sin\alpha_g\big|_{v=0}, \quad (12)$$

where h_{12} is the head difference between stations 1 and 2, α_g the slope angle of the pressure gauge, h_{s1} the relative head at station 1, and h_{s2} the relative head at station 2. The air supply measuring the cylinder can provide a desired air quantity under atmospheric conditions. For example, if an air volume V_0 is needed, the equipment is operated as follows: (1) close valve #1 and open valve #2; (2) lower the removable cylinder until the air in the fixed cylinder is V_0; (3) close valve #2 and raise the removable cylinder to a reasonable level, and then open valve #1 until all air is injected into the hump pipe.
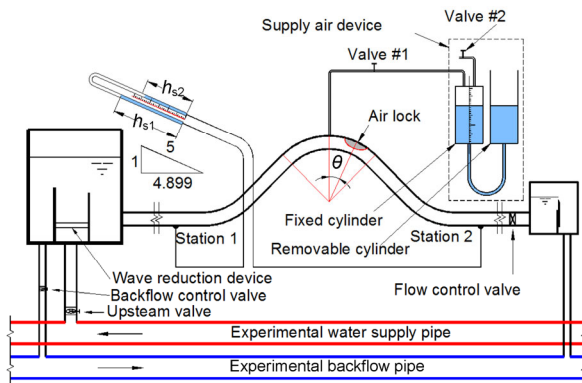

Fig. 5 Schematic of the experimental principle

Fig. 6 Experimental facilities in the field

In the experiment, the upstream water level can be set by the backflow control valve, and the flow discharge is set by the flow control valve. A tapeline

adhered to the external surface of the hump pipe marks the external arc length. Accordingly, the central angle of the air pocket is

$$\theta = 0.5\pi(l_u + l_d)/R_b, \quad (13)$$

where l_u is the left arc length of the air pocket, l_d the right arc length of the air pocket, and R_b the external radius of the hump.

4 Experimental analysis and empirical fitting

Fig. 7 shows a typical air lock observed in the hump pipe zone in the experiment. These air pockets are separately 40, 80, and 160 cm^3, the corresponding equivalent radii are respectively 0.021, 0.027, and 0.034 m, and the flow velocity varies from 0 to 0.6 m/s.
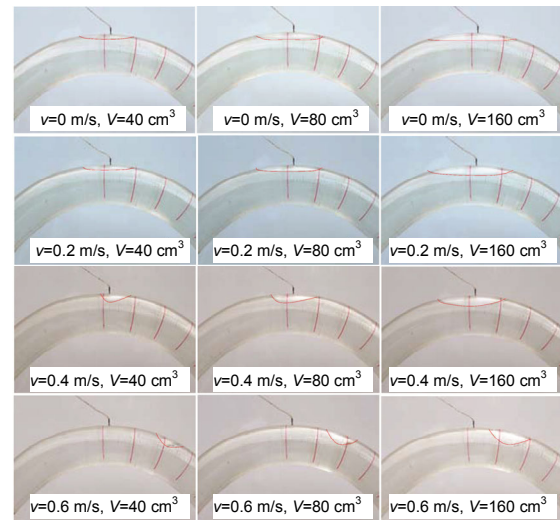

Fig. 7 Typical air lock patterns in a hump pipe zone

As seen in these pictures, the partial air lock can occur near the top of the hump. With the increase of the pipe flow velocity, the air pockets go downstream and spill from the outlet. In other words, if the drag force is large enough to move the air pocket at the maximum depression angle, it can entirely remove the air pocket from the hump pipe zone.

To analyze the influence of the air lock on the flow capacity of the pipe, extra head losses caused by the air lock are analyzed based on the measured

results. Various air volumes are used to investigate the resistance properties of the trapped air pocket in the hump pipe. Considering a dimensionless format, a maximum equivalent sphere ($\tilde{r} = 1$) is chosen as a reference. The corresponding length of the air column is $h_0 = 4r_0/3$. Considered as the velocity head $h_0 = v_0^2/(2g)$, the corresponding velocity is $v_0 = (2gh_0)^{1/2}$. Fig. 8 shows the dimensionless head losses between station 1 and station 2 for four kinds of conditions, where the air pocket volumes are separately 0 (without trapped air pocket), 40, 80, and 160 cm^3. The dimensionless scales of the air pockets for the last three kinds of conditions are separately $\tilde{r} = 0.472$, 0.594, and 0.748.

In fact, it is difficult to measure directly the head losses caused by the air pocket, since they are always coupled with the friction and minor losses of the hump pipe. Usually, the extra head losses can be determined by the subtraction of the original head losses without air pockets from the total head losses with air pockets. As seen in Fig. 8, all the measured data are presented as scatters. Considering the alternation of laminar and turbulent flows during the increase of flow velocity, the general head losses can be expressed as follows:

$$h_f = f\left(\frac{64}{vd/v}, \lambda_t\right)\frac{l_{12}}{d}\frac{v^2}{2g}, \tag{14}$$

where f is a function symbol, d the internal diameter of the pipe, v the kinematic viscosity, l_{12} the pipe length between stations 1 and 2, and λ_t the Darcy friction factor in turbulent flow which can be determined by the Colebrook formula (Finnemore and Franzini, 2002):

$$\frac{1}{\sqrt{\lambda_t}} = -2\log\left(\frac{e}{3.7d} + \frac{2.51}{Re\sqrt{\lambda_t}}\right),$$

in which e is the roughness coefficient and Re the Reynolds number. Define dimensionless head losses $\tilde{h}_f = h_f/h_0$, dimensionless velocity $\tilde{v} = v/v_0$, laminar head loss coefficient $K_1 = \dfrac{64}{v_0 d/v}\dfrac{l_{12}}{d}C_1$, and turbulent head loss coefficient $K_2 = \lambda_t\dfrac{l_{12}}{d}C_2$, where C_1

and C_2 are constant coefficients. For the original head losses without the air lock, a polynomial function through the origin of coordinates can be expressed as

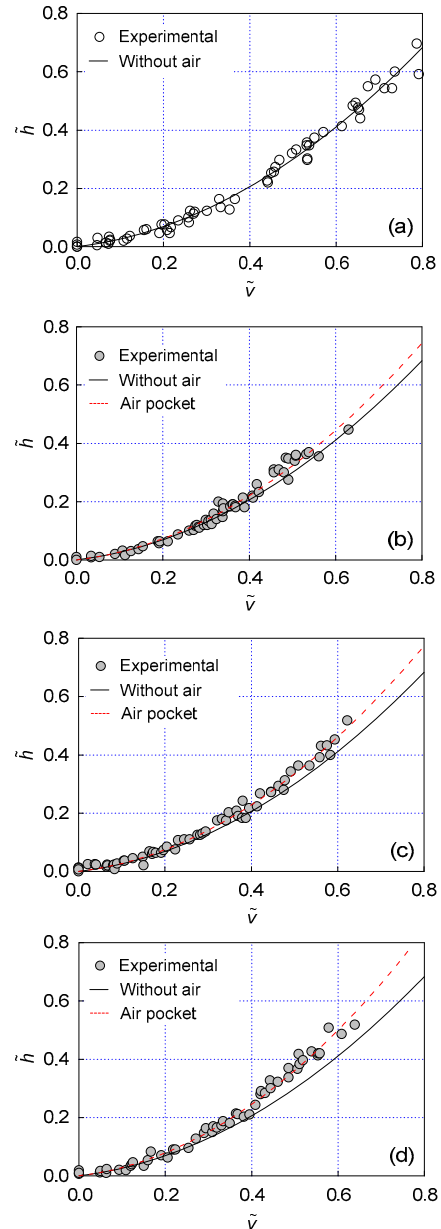$$\tilde{h}_f = K_1\tilde{v} + K_2\tilde{v}^2. \tag{15}$$

Fig. 8 Hydraulic head losses between station 1 and station 2

(a) Air pocket volume is 0, without trapped air pocket; (b) Air pocket volume is 40 cm^3, $\tilde{r} = 0.472$; (c) Air pocket volume is 80 cm^3, $\tilde{r} = 0.594$; (d) Air pocket volume is 160 cm^3, $\tilde{r} = 0.748$

The head losses induced by the air pocket are considered as a minor head loss $\tilde{h}_a = K_a \tilde{v}^2$, where K_a is the head loss coefficient of an air lock. Then the dimensionless entire head losses can be written as

$$\tilde{h} = K_1 \tilde{v} + K_2 \tilde{v}^2 + K_a \tilde{v}^2. \tag{16}$$

Based on the experimental data of the original head losses without air pocket, coefficients K_1 and K_2 can be determined by the method of least squares in Eq. (15). Then according to Eq. (16), coefficient K_a of extra head losses can be determined for various scale-trapped air pockets. The coefficients are presented in Table 1.

Table 1 Extra head loss coefficients for various volumes

K_1	K_2	K_a		
		$\tilde{r} = 0.472$	$\tilde{r} = 0.594$	$\tilde{r} = 0.748$
0.175	0.849	0.094	0.141	0.247

In Fig. 8, the solid lines show the fitting curves of the flow velocities with head losses without air locks, which are consistent with Eq. (15). In this study, they are considered as the references for extra head losses of the air lock. The dash lines are the fitting curves of the head losses with air pockets. As shown in the figure, these curves are steeper than the reference line. In other words, head losses with air locks are generally larger than those without air locks. Considering the same conditions, a larger trapped air pocket always brings more extra head losses. In fact, the extra head losses due to air locks are only a part of the minor losses. To analyze the extra head losses, the fitting head loss line without an air lock is selected as the reference.

According to these coefficients, it is shown that the head losses increase with the increase of the trapped air volume. The lines in Fig. 9 show separately the extra head losses caused by various air locks. These results show that the air lock can increase the resistance to the flow in the hump pipe zone. The resistance increases with the increase of the flow velocity and the volume of the air lock. According to dimensional analysis, it is proportional to the second power of the pipe flow velocity, and the coefficient increases with the increase of the volume of the air lock. In summary, the above analysis shows that air locks can cause extra head losses in closed pipe flow. Under the same conditions, the extra head losses increase with the increase of air volumes and pipe flow velocities.

In fact, the trapped air pocket deforms and splits with the pipe flow patterns. Therefore, the experiment refers particularly to a macro-scale trapped air pocket. As shown in Fig. 4, the location of the air lock is defined by three angles, i.e., α, β, and θ, where $\theta = (\alpha + \beta)/2$. As the hump radius is very large in comparison with the air lock, the three angles are similar in magnitude. Thus, the mean angle θ is chosen to represent approximately the location of the air lock. The experimental scatters in Fig. 10 show the location angles of the air lock with various pipe flow velocities and volumes. As seen in the figure, the location slope angle increases significantly with the increase of the flow velocities and decreases slightly with the increase of the volumes.
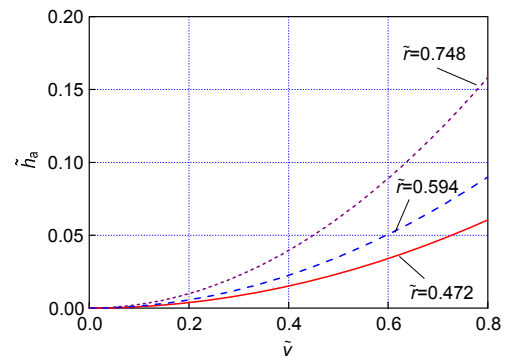
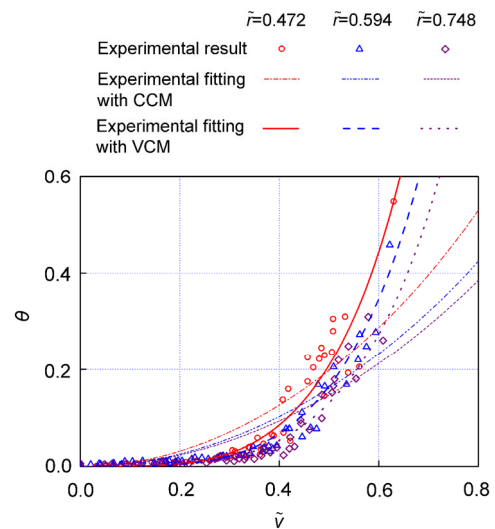

Fig. 9 Extra head losses caused by air locks

Fig. 10 Influence of the flow velocity on the location of an air lock

According to Eq. (9), defining dimensionless density ratio $\tilde{\rho} = \rho_\mathrm{w}/(\rho_\mathrm{w} - \rho_\mathrm{a})$, and substituting variable $\theta' = \sin\theta$, the general location of the critical equilibrium conditions can be expressed as the dimensionless format:

$$\theta' = C_\mathrm{D}^* \tilde{\rho} \frac{\tilde{v}^2}{\tilde{r}}. \qquad (17)$$

Accordingly, the coefficients can be determined based on the experiments for a constant volume:

$$M'_{C_\mathrm{D}^*} = \sum_{i=1}^{n} \left[\tilde{\rho} \frac{\tilde{v}_i^2}{\tilde{r}} \left(C_\mathrm{D}^* \tilde{\rho} \frac{\tilde{v}_i^2}{\tilde{r}} - \theta_i' \right) \right], \qquad (18)$$

$$C_\mathrm{D}^* = C_\mathrm{D}^* \big|_{M'_{C_\mathrm{D}^*}=0}, \qquad (19)$$

where $M'_{C_\mathrm{D}^*}$ is a squared residual, subscript i the experimental serial number, and n the total number of the experimental data. Considering C_D^* as a constant coefficient model (CCM), Eq. (19) is consistent with the least squares method. However, it is very difficult to solve directly. Here, a clamp trial method is used to solve coefficient C_D^* by a computer program. Table 2 shows the coefficients for various air volumes by the CCM.

Table 2 Coefficients for various air volumes

$\tilde{r}$	C_D^*
0.472	0.372
0.594	0.382
0.748	0.440

These fittings show, for an equivalent sphere, that the drag coefficients are about 0.4. The corresponding curves can be drawn in Fig. 10. As seen in the figure, these curves meet the dimensional principle; however, they obviously distort the experimental results. In fact, the fitting curves can be greatly improved if the influence of the flow patterns is considered by coupling the Reynolds number. To still comply with the above dimension concordant principle, the Reynolds number is considered as an independent factor coupled with the drag coefficient. Considering C_D^* as a variable coefficient model (VCM), which depends on the Reynolds number, the proposed drag coefficient is written as

$$C_\mathrm{D}^* = K_\mathrm{d} Re^k, \qquad (20)$$

where K_d and k are constant coefficients, and $Re = vd/\nu$. Then

$$\theta' = K_\mathrm{d} Re^k \tilde{\rho} \frac{\tilde{v}^2}{\tilde{r}}. \qquad (21)$$

To obtain the optimal sets of k and K_d, considering θ' and Re as the data sets in Eq. (21), for a specific k, a matched K_d and the corresponding squared residual M can be determined. Fig. 11 shows that the squared residual varies with the sets of k and K_d. The optimal set is determined at the point with the minimum squared residual M_min.
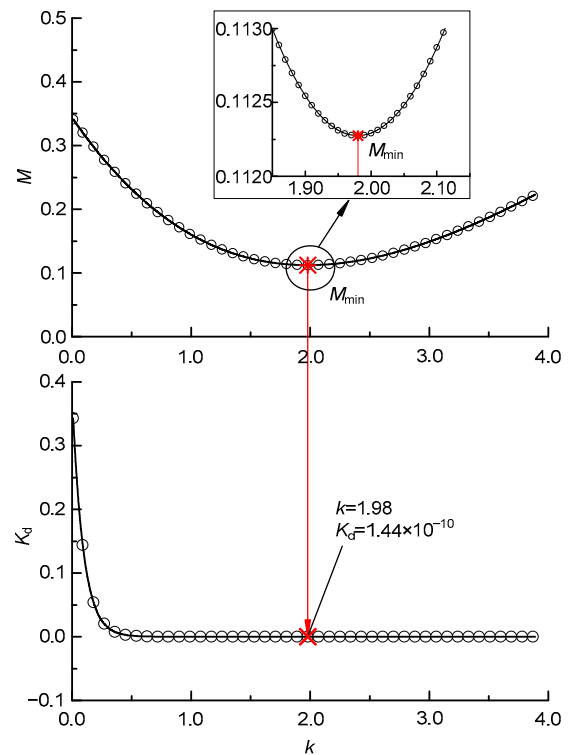

Fig. 11 Squared residuals and the sets of k and K_d

Based on the optimal sets of k and K_d in Table 3, the final empirical formula can be written as

Table 3 Optimal coefficient sets and the squared residual

k	K_d	M
1.98	1.44×10^{-10}	0.112

$$\theta = \arcsin\left(K_{\mathrm{d}}Re^{k}\tilde{\rho}\frac{\tilde{v}^{2}}{\tilde{r}}\right). \tag{22}$$

Accordingly, the revised curves are shown in Fig. 10. Obviously, after considering the influence of the flow patterns, these fitting curves are better approximations to the experimental results. As shown in the figure, the revised curve can represent the distribution principle of the location slope angles with the pipe flow velocities and air volumes. The equilibrium angle increases significantly with the increase of the flow velocity, but it decreases slightly with the increase of the air volume. The above result shows that it is more difficult to remove trapped air from a large-slope angle pipe than from a gentle incline pipe. In other words, a greater flow velocity and a smaller pipe depression angle are needed to avoid an undesired air lock in the hump zone of a water supply pipeline system.

5 Prevention and elimination of an air lock in a hump pipe

As is known, an air lock can bring undesired head losses and failure risk for closed pipe flow. Therefore, it is important to design so as to prevent potential air locks in a long-distance water supply pipeline system. The above research shows that the flow velocity, the pipe slope, and the volume of the trapped air pocket, can greatly affect the critical equilibrium of an air lock in a hump pipe zone.

In the experiment, with the increase of the pipe flow velocity, the trapped air moves to a new equilibrium location with a larger slope angle to resist the drag force. Practically, a trapped air pocket will move downstream if the pipe velocity increases and exceeds the critical velocity of the maximum slope angle in the hump zone. As shown in Fig. 10, the equilibrium angle increases with the increase of the pipe flow velocity. The trapped air is entirely removed when the flow exceeds the critical flow velocity for the maximum slope angle.

In the design stage, it is important for the designer to choose the pipe slope and pipe flow velocity. According to Eq. (22), there are two approaches to prevent an air lock in an irregularly undulating submarine water supply pipeline system. One is increasing the pipe flow velocity, and the other is decreasing the maximum slope angle of the pipeline. For a specified velocity, the allowable critical slope angle can be determined by

$$\theta_{\max} = \arcsin\left(K_{\mathrm{d}}Re^{k}\tilde{\rho}\tilde{v}_{\mathrm{c}}^{2}/\tilde{r}\right). \tag{23}$$

To avoid an air lock, the slope angle at any point should be smaller than the critical slope.

As shown in the above research, besides the pipe flow velocity, the air volume can slightly affect the equilibrium location. For example, to prevent a 160-cm^3 air pocket in the experimental pipe system, the allowable maximum slope angles are determined by Eq. (23) for various specified flow velocities. Fig. 12 shows the different operating zones. The solid line is the critical equilibrium line, where K_{c} is a criterion coefficient. The upper operating zone may cause a potential air lock and the lower operating zone can prevent an air lock. In other words, the maximum slope angle should be smaller than the critical slope angle to prevent an air lock.
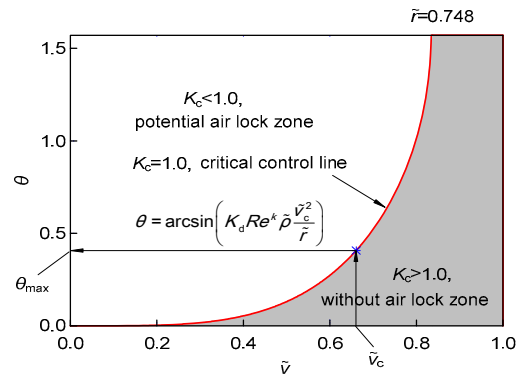

Fig. 12 Operating zones for the prevention of trapped air dissipation

Considering the effects of the trapped air volumes, Fig. 13 shows the effect of the trapped air volume on the critical slope line. As shown in this figure, the volume can affect the equilibrium slope angle, which increases with the increase of the volume. To prevent a larger air pocket, a greater velocity or a smaller slope angle is needed.

An existing air lock can bring extra head losses and potential hazards in a water supply pipeline. It is important to remove the existing air lock during operation. As presented in the above analysis, for a given slope angle, the pipe flow velocity can greatly

affect the air lock equilibrium. The trapped air pocket can move downstream if the pipe flow velocity is large enough. For a given pipe system, according to Eq. (23), the dimensionless critical flow velocity $\tilde{v}_c$ for removing the air pocket can be expressed as

$$\tilde{v}_c = \sqrt{\frac{\tilde{r}}{K_d Re^k \tilde{\rho}} \sin\theta_{max}}, \qquad (24)$$

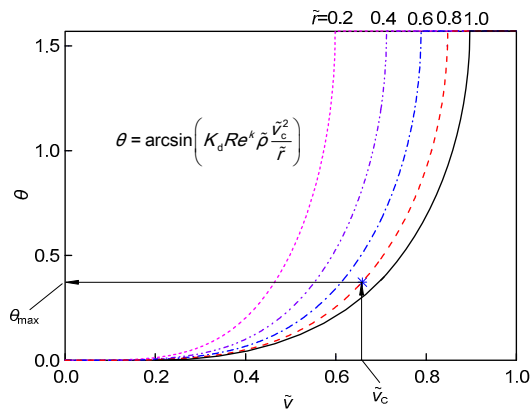where θ_{max} is the allowable maximum depression angle.

Fig. 13 Effect of trapped air volume on the critical slope lines

Practically, the existing air pocket can be removed by running a higher pipe flow velocity temporarily. Fig. 14 shows the critical flow velocity line for a specific air volume. As shown in the figure, the critical velocity increases with the increase of the slope angle. For a known pipeline, the critical velocity depends on the maximum slope angle. If an air lock occurs in a practical project, it can be removed by operating at a greater velocity than the critical one for a short period.

Analogously, Fig. 15 shows the effect of the trapped air volume on the critical velocity line. As shown in this figure, the critical velocity increases with the increase of the air volume, which shows that a greater velocity is needed to remove a larger air pocket.

To predict or evaluate the possibility of an air lock in an irregular undulating submarine water supply pipeline system, a simple evaluation criterion is proposed. According to the critical equilibrium of the trapped air pocket in the hump pipe zone, the criterion coefficient can be expressed as follows:

$$K_c = \frac{K_d Re^k \tilde{\rho} \tilde{v}_c^2}{\tilde{r} \sin\theta_{max}}. \qquad (25)$$

The coefficient represents the relationship among the operating flow velocity, the maximum slope angle, and the possible air pocket scale in the hump pipe zone. The pipe system will not trap an air pocket in the hump zone when the coefficient is greater than 1.0. Conversely, the hump zone can trap potential air and accumulate a partial air lock. Obviously, a greater flow velocity and a less depression angle are advantageous in avoiding air locks, since they both can increase the criterion coefficient.
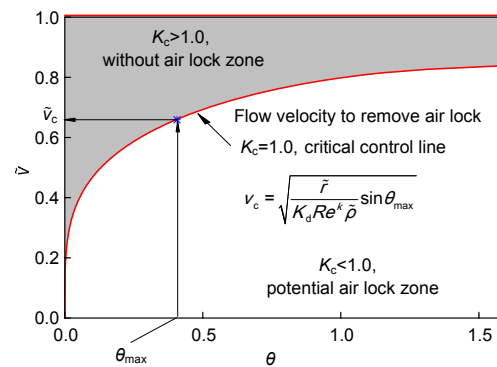

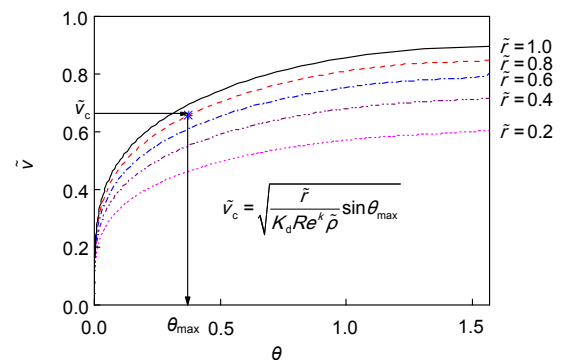**Fig. 14 Critical flow velocity to remove trapped air pocket**

Fig. 15 Effect of the trapped air volume on the critical velocity line

6 Analysis and discussion

As an undesired phenomenon in water supply pipeline systems, air locks can restrict flow and even

cause pipe burst. Thus, it is important to protect pipes against air lock hazards. In an annular pipe, the experiment simulates the movement of the trapped air pocket in the hump zone of a submarine water supply pipeline system. A hump air lock can decrease the flow section and capacity of a water supply pipeline system. The volume of the trapped air pocket plays an important role in hydraulic head losses. Generally, a larger trapped air pocket can bring greater extra head losses, and it is more difficult to remove the air pocket from the hump zone. Based on the experimental measurement and the ESM, the extra head loss is analyzed and it can be considered as a minor head loss. For the critical equilibrium, the pipe flow velocity can greatly affect the critical slope angle of the air lock in the hump zone, but the air volume only slightly affects the critical angle of the air lock. To avoid air lock hazards in submarine water supply pipelines, some designers may seek to employ an excess velocity and a small slope angle. In fact, it is essential and easy to avoid air locks in hump zones by using the proposed criterion coefficient. The investigation analyzes only the macroscopic movement of the air pocket as an entire mass. In fact, some small bubbles may separate from the trapped air mass and move downstream with the pipe flow before the trapped air pocket reaches the critical flow velocity.

7 Conclusions

An air lock can cause extra head losses and decrease the local flow section; consequently, it decreases the flow capacity of a water supply pipeline. ESM is proposed to simplify the air lock patterns. The head losses increase with the increase of the pipe flow velocity and the volume of the air lock, and can be considered as minor losses. The pipe flow velocity has a great influence on the critical equilibrium of the trapped air pocket in the hump pipe zone. The critical equilibrium angle increases and the air lock moves downstream to a new equilibrium location with an increasing pipe flow velocity. There are two approaches to prevent potential air locks. One is increasing the pipe flow velocity, and the other is decreasing the maximum slope angle of the pipe. A criterion coefficient is proposed to evaluate the possibility of an air lock. According to this criterion, a

greater flow velocity and a less depression angle are advantageous to avoid the air lock hazard in a submarine water supply pipeline system. It can be a reference for preventing or estimating the partial hump air lock in the design and operation of submarine water supply pipelines.

References

Brown, L., 2006. Understanding Gravity-Flow Pipelines Water Flow, Air Locks and Siphons. http://www.itacanet.org/understanding-gravity-flow-pipelines-water-flow-air-locks-and-siphons/

Burch, T.M., Locke, A.Q., 2012. Air lock and embolism upon attempted initiation of cardiopulmonary bypass while using vacuum-assisted venous drainage. *Journal of Cardiothoracic and Vascular Anesthesia*, **26**(3):468-470. http://dx.doi.org/10.1053/j.jvca.2011.01.019

Burrows, R., Qiu, D.Q., 1995. Effect of air pockets on pipeline surge pressure. *Proceedings of the Institution of Civil Engineers-Water, Maritime and Energy*, **112**(4):349-361. http://dx.doi.org/10.1680/iwtme.1995.28115

Carlos, M., Arregui, F.J., Cabrera, E., *et al.*, 2011. Understanding air release through air valves. *Journal of Hydraulic Engineering*, **137**(4):461-469.

Chaiko, M.A., Brinckman, K.W., 2002. Models for analysis of water hammer in piping with entrapped air. *Journal of Fluids Engineering-Transactions of the ASME*, **124**(1):194-204. http://dx.doi.org/10.1115/1.1430668

Epstein, M., 2008. A simple approach to the prediction of waterhammer transients in a pipe line with entrapped air. *Nuclear Engineering and Design*, **238**(9):2182-2188. http://dx.doi.org/10.1016/j.nucengdes.2008.02.023

Escarameia, M., 2007. Investigating hydraulic removal of air from water pipelines. *Proceedings of the Institution of Civil Engineers-Water Management*, **160**(1):25-34. http://dx.doi.org/10.1680/wama.2007.160.1.25

Ferreri, G.B., Ciraolo, G., Lo Re, C., 2014. Storm sewer pressurization transient—an experimental investigation. *Journal of Hydraulic Research*, **52**(5):666-675. http://dx.doi.org/10.1080/00221686.2014.917726

Finnemore, E., Franzini, J., 2002. Fluid Mechanics with Engineering Applications (10th Edition). McGraw-Hill Education, Boston, USA, p.261-284.

Greenshields, C.J., Leevers, P.S., 1995. The effect of air pockets on rapid crack propagation in PVC and polyethylene water pipe. *Plastics, Rubber and Composites Processing and Applications*, **24**(1):7-12.

Izquierdo, J., Fuertes, V.S., Cabrera, E., *et al.*, 1999. Pipeline start-up with entrapped air. *Journal of Hydraulic Research*, **37**(5):579-590. http://dx.doi.org/10.1080/00221689909498518

Lin, C., Liu, T., Yang, J., *et al.*, 2015. Visualizing conduit flows around solitary air pockets by FVT and HSPIV. *Journal of Engineering Mechanics*, **141**(5):04014156

http://dx.doi.org/10.1061/(asce)em.1943-7889.0000867

Liu, T., Yang, J., 2013. Experimental studies of air pocket movement in a pressurized spillway conduit. *Journal of Hydraulic Research*, **51**(3):265-272.
http://dx.doi.org/10.1080/00221686.2013.777371

Pothof, I., Clemens, F., 2010. On elongated air pockets in downward sloping pipes. *Journal of Hydraulic Research*, **48**(4):499-503.
http://dx.doi.org/10.1080/00221686.2010.491651

Pothof, I., Clemens, F., 2011. Experimental study of air-water flow in downward sloping pipes. *International Journal of Multiphase Flow*, **37**(3):278-292.
http://dx.doi.org/10.1016/j.ijmultiphaseflow.2010.10.006

Pozos, O., Gonzalez, C.A., Giesecke, J., *et al.*, 2010. Air entrapped in gravity pipeline systems. *Journal of Hydraulic Research*, **48**(3):338-347.
http://dx.doi.org/10.1080/00221686.2010.481839

Pozos-Estrada, O., Fuentes-Mariles, O.A., Pozos-Estrada, A., 2012. Gas pockets in a wastewater rising main: a case study. *Water Science and Technology*, **66**(10):2265-2274.
http://dx.doi.org/10.2166/wst.2012.462

Pozos-Estrada, O., Pothof, I., Fuentes-Mariles, O.A., *et al.*, 2015. Failure of a drainage tunnel caused by an entrapped air pocket. *Urban Water Journal*, **12**(6):446-454.
http://dx.doi.org/10.1080/1573062x.2015.1041990

Reynolds, C., Yitayew, M., 1995. Low-head bubbler irrigation systems. Part II: Air lock problems. *Agricultural Water Management*, **29**(1):25-35.
http://dx.doi.org/10.1016/0378-3774(95)01189-7

Vasconcelos, J.G., Leite, G.M., 2012. Pressure surges following sudden air pocket entrapment in storm-water tunnels. *Journal of Hydraulic Engineering*, **138**(12):1081-1089.

Yu, Y., 2015. Study of Critical Characteristic of Hump Air Resistor in Submarine Water Supply Pipeline. MS Thesis, Zhejiang University, Hangzhou, China (in Chinese).

Zhou, F., Hicks, F., Steffler, P., 2004. Analysis of effects of air pocket on hydraulic failure of urban drainage infrastructure. *Canadian Journal of Civil Engineering*, **31**(1):86-94.
http://dx.doi.org/10.1139/l03-077

Zhou, L., Liu, D.Y., Karney, B., 2013. Investigation of hydraulic transients of two entrapped air pockets in a water pipeline. *Journal of Hydraulic Engineering*, **139**(9):949-959.
http://dx.doi.org/10.1061/(asce)hy.1943-7900.0000750

中文概要

题　目：供水管路中驼峰气阻的临界平衡实验研究

目　的：输水管道的驼峰气阻是指由于管路高峰位置的滞气作用使气体不断聚积在峰顶附近、产生的气体阻碍水流的局部水力现象。它能够导致管路过水断面减小、输水能耗增加、输送效率降低和管路压力振荡等后果，严重威胁海底管道输水的稳定性和安全性。本文旨在分析滞留气团在供水管道中的力学平衡、能量损失、移动和溢出机理，研究水流流速对气团的推移特性，提出预测和消除驼峰气阻的方法，使输水管道免受驼峰气阻的危害，提高输水管道的供水效率。

创新点：1. 设计了具有连续坡角变化的圆弧形驼峰管道实验，该实验可以定量模拟气团体积和平衡角度；2. 建立了驼峰气阻的水头损失经验公式和恒定流情况下驼峰气阻的管道坡角和流速的对应关系式，可用于预测和消除驼峰气阻的危害。

方　法：1. 通过驼峰气团的受力特性分析，获得满足量纲和谐的力学平衡方程；2. 采用试验观察和测试获得有无气泡情况下的水头损失和平衡状态下的坡角，通过等价球体方法对测试数据进行无量纲拟合，获得气阻的水头损失方程系数，并通过流速和平衡坡角建立恒定流情况下的临界平衡方程；3. 基于试验拟合获得临界平衡方程，建立预测和评估气阻的准则系数，并提出消除气阻的水流临界流速。

结　论：1. 当管路流速较小时，供水管路的驼峰顶端可能滞留和聚集气体，形成驼峰气阻；气体体积越大对水流阻碍越明显，可能造成的水头损失也越大；2. 利用等价球体法可以极大地简化驼峰气阻的形状，并良好地模拟气阻的平衡特性和阻力特性；3. 管道流速是影响驼峰气阻临界平衡位置的最重要因素，通过减小管道起伏的坡角或增加水流流速可以防止和消除驼峰气阻的危害。

关键词：驼峰管道；管流；滞留气团；水力试验；供水管道